Journal of Nuclear Materials 390–391 (2009) 183–187

Contents lists available at ScienceDirect

Journal of Nuclear Materials

journal homepage: www.elsevier.com/locate/jnucmat

Molecular dynamics simulation of hydrogen atom sputtering on the surface of graphite with defect and edge

Atsushi Ito [a,c,*], Ying Wang [a], Stephan Irle [a,c], Keiji Morokuma [b], Hiroaki Nakamura [c]

[a] *Nagoya University, Nagoya 464-8602, Japan*
[b] *National Institute for Fusion Science, Toki 509-5292, Japan*
[c] *Kyoto University, Kyoto 606-8103, Japan*

ARTICLE INFO

PACS:
81.05.T
71.15.D
79.20.R
61.72.J

ABSTRACT

We report effects of graphite vacancy and hydrogen isotopes in chemical sputtering due to hydrogen atoms onto graphite surfaces by use of molecular dynamics simulation. A modified Brenner reactive empirical bond order potential, which was benchmarked using *ab initio* CCSD(T) and hybrid DFT potential energy curves, was used to compute energies and gradients during the MD simulations. Interlayer intermolecular interaction between layers of graphite was represented by original potential model. By the injection of hydrogen atoms, a graphite of perfect crystal was peeled off one by one from a surface clearly, while a graphite including vacancies was amorphized simultaneously. The graphite including monovacancies was amorphized more strongly than graphite including divacancies. Flux of carbon atoms detached from the surface by hydrogen atom bombardment increases linearly as incident energy increases. The effects of isotope is that the time at which the hydrogen atom bombardment start producing hydrocarbon molecules increases as the mass of a hydrogen isotope increases.

1. Introduction

In the scene of plasma confinement of nuclear fusion, polycrystalline graphite and carbon fiber composite are used as divertor plate and they experience the bombardment of hydrogen plasma. Experiments have reported that the surfaces of the divertor tiles were eroded and then hydrocarbon molecules were generated. The hydrocarbon molecules are undesirable impurities in plasma confinement and cause a problem of the deposition of carbon dust. Thus, plasma–wall interaction should be understood in erosion process. As a theoretical approach, molecular dynamics (MD) simulation has been used to clarify the erosion process from dynamics in atomic scale.

A graphite material is supported by plural kinds of forces and it has a hierarchic structure. The smallest level, that is one molecule, is a sheet structure called graphene. The graphene consists of carbon atoms combined by sp^2 covalent bonds. The next level of a graphite material is single crystal graphite. The single crystal graphite has a layer structure stacking graphenes to 'ABAB' or 'ABC' order. These graphenes are supported by interlayer intermolecular forces. Last level of a graphite material is polycrystalline graphite. The polycrystalline graphite consists of clusters of the single crystal graphite. The target of the present MD simulation is the single crystal graphite. Then we need the model of two kinds of forces, the force by covalent bond and the interlayer intermolecular force.

We have developed methods to treat a graphite material with hydrogen atom step by step. To represent the covalent bond, that is here C–C, C–H and H–H bonds, we use the Brenner reactive empirical bond order (REBO) potential from 2002 [1] where we modified some parameters and functions related to potential energy curve between carbon and hydrogen atoms and numerical accuracy in difference equation [2,3], which is here called a modified Brenner REBO potential.

Next, we have proposed a compatible potential model for the interlayer intermolecular forces with the modified Brenner REBO potential and then the single crystal graphite composed of graphene layers can be treated in MD simulation [3].

A real graphite material has defects and edges. Because large defects and large edges relate to the polycrystalline graphite, MD has not been able to treat them yet. However, a vacancy in graphite lattice can be regarded as the smallest defect and has the smallest zigzag or armchair edges. In the present paper, we report the effects of vacancies in the single crystal graphite bombarded by hydrogen atoms. Two kinds of vacancies, monovacancies and divacancies, are treated. Moreover, injections of deuterium and tritium are also tried and their differences in hydrocarbon production are researched.

---

* Corresponding author. Present address: Department of Simulation Science, National Institute for Fusion Science, Oroshi-cho 322-6, Toki 509-5292, Japan.
E-mail address: ito.atsushi@nifs.ac.jp (A. Ito).

0022-3115/$ - see front matter © 2009 Elsevier B.V. All rights reserved.
doi:10.1016/j.jnucmat.2009.01.163

2. Simulation method

The physical system treated by MD simulation is described here. Incident particles were injected perpendicular to graphite (0001) surfaces at intervals of 0.1 ps and the incident flux was 2.5×10^{30} atom/m^2 s. To show the effect of hydrogen isotope, three kinds of particles, hydrogen, deuterium and tritium atoms, were prepared. We simulated at the incident energies 2–30 eV. We knew that these incident energies causes different interactions between a single graphene sheet and a single hydrogen isotopes in MD simulations [4,5]. Also in the dynamics of hydrogen atoms in layered graphite, the incident energies of 5 eV, 15 eV and 30 eV brought about adsorption on the top layer, reflection by the top layer and intercalation between graphite layers. In the MD simulations, the incident energy E_{I} determined the initial momentum of the incident particle as $\sqrt{2mE_{\mathrm{I}}}$, where m was the mass of the incident particle, 1 u, 2 u and 3 u for hydrogen, deuterium and tritium atoms, respectively. The initial x and y coordinates of the incident particle were set at random. The initial z coordinate of the incident particle was at a distance of 4.83 nm from the graphite surface.

The graphite of single crystal here consisted of eight layers and had a structure of 'ABAB' stacking. The graphite (0001) surface faced the positive z-direction. The layers were parallel to the x and y surface. Each layer was graphene which consisted of 160 carbon atoms measuring 2.00×2.17 nm^2. The size of the simulation box in the x- and y-directions was equal to that of the graphenes with periodic boundary conditions. The initial interlayer distance of the graphite was 3.35 Å. The graphenes were numbered from the surface, e.g. the first graphene. During the simulation, two carbon atoms of the eighth graphene were fixed to prevent the graphite from moving. To investigate the dependence on lattice vacancies, three kinds of graphites were treated. One graphite had a structure of perfect crystal, and the others had monovacancies or divacancies (see Fig. 1). In the graphite including vacancies, each graphene layer had eight monovacancies or four divacancies, hence, the two kinds of graphite including vacancies had same carbon density. The carbon atoms obeyed the Maxwell–Boltzmann distribution at 300 K initially.

In the present simulation, two kinds of potential models were used to deal with chemical interaction at short distance and intermolecular interaction at long distance. Chemical interaction was represented by the modified Brenner REBO potential [2,3], which is created by the modification of the parameter and function on the basis of the original Brenner REBO potential from 2002 [1]. In the potential models, the existence of a covalent bond was judged by the distance between two atoms. C–C and C–H bonds appear when a distance between atoms was less than 2.0 Å and 1.8 Å, respectively.

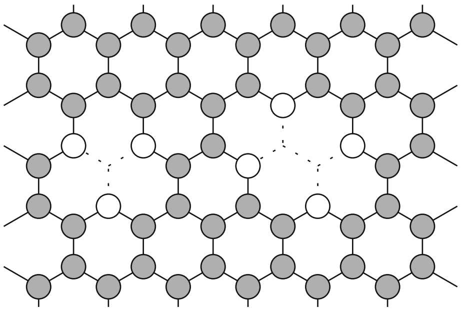

Fig. 1. The monovacancy (left) and the divacancy (right) in the graphene lattice. Spheres indicate carbon atoms. Especially, white sphere is instable carbon atom, which has only two covalent bonds.

We note the following important information. In the modified Brenner REBO potential and the original Brenner REBO potential from 2002, small potential barrier of 0.4–0.5 eV on the potential energy curves (PECs) between a hydrogen atom and a graphene surface at a distance 1.6–1.9 Å appears. This small potential barrier causes the reflection of a hydrogen atom from a graphene surface for the incident energy less than 1 eV [2]. However, the Brenner REBO potential from 1990 [6] does not show the small potential barrier.

The potential model should be checked against interaction potentials from high-level quantum chemical methods. For this purpose we compared the PECs between the carbon atom of an infinite graphene layer and a hydrogen atom from the modified Brenner REBO with PECs for coronene and pyrene model compounds treated at hybrid B3LYP density functional theory (DFT) and coupled-cluster CCSD(T) levels of theory. We employed Dunning's correlation-consistent cc-pVDZ basis set. It was found that RCCSD(T)//B3LYP energies, which are computationally very expensive, are surprisingly close to straightforward B3LYP energies, which can be obtained at a fraction of the computational cost. The modified REBO potential and *ab initio* and DFT calculations agree that an entrance channel barrier of about 0.4–0.5 eV exists, and the similarity of the PECs for both pyrene and coronene suggest that the H–C interaction is very localized. These results will be reported in greater detail elsewhere.

The interlayer intermolecular potential kept the interlayer distance of the graphite 3.35 Å and produced the 'ABAB' stacking. To use the interlayer intermolecular potential with the modified Brenner REBO potential, a special cutoff function is proposed. In an idea of the special cutoff function, the interlayer intermolecular potential was valid at only the outside of a cone made centering on a covalent bond. The details of the interlayer intermolecular potential and the special cutoff function were written in our previous paper [3].

The second-order symplectic integration [7] was used to solve the time evolution of the equation of motion; the time step was 5×10^{-18} s. The MD simulations were performed under the *NVE* condition, in which the number of particles (N), volume (V), and total energy (E) were conserved, i.e. the temperature of the graphite is not controlled.

3. Result

The MD simulation treated three cases of single crystal graphite to investigate the dependency on vacancies. One was a graphite of perfect crystal and the others were graphites including monovacancies or divacancies.

When the hydrogen atoms were injected into the graphite of perfect crystal, snapshots from the MD simulation illustrated the layers of graphite was peeled off one by one from the surface (see Fig. 2). This phenomenon is here called 'graphite peeling'. Peeled graphenes broke into small hydrocarbon molecules having mainly chain structures and the layer structure of under graphenes was maintained.

Before graphite peeling occurred, the hydrogen atoms retention depend on the incident energy as follows. In the case of the incident energy of 5 eV, hydrogen atoms were adsorbed by the first graphene. In the case of 15 eV, hydrogen atoms mainly reflected by the first graphene. In the case of 30 eV, intercalation of hydrogen atom between the first and second graphenes occurred.

On the other hand, in the case of graphite including vacancies, the intercalation of hydrogen atom occurred independently of the incident energy. In addition, the graphite peeling is not clear against to the case of perfect crystal. In other words, the peeled graphene remained debris on the next graphene layer. The most

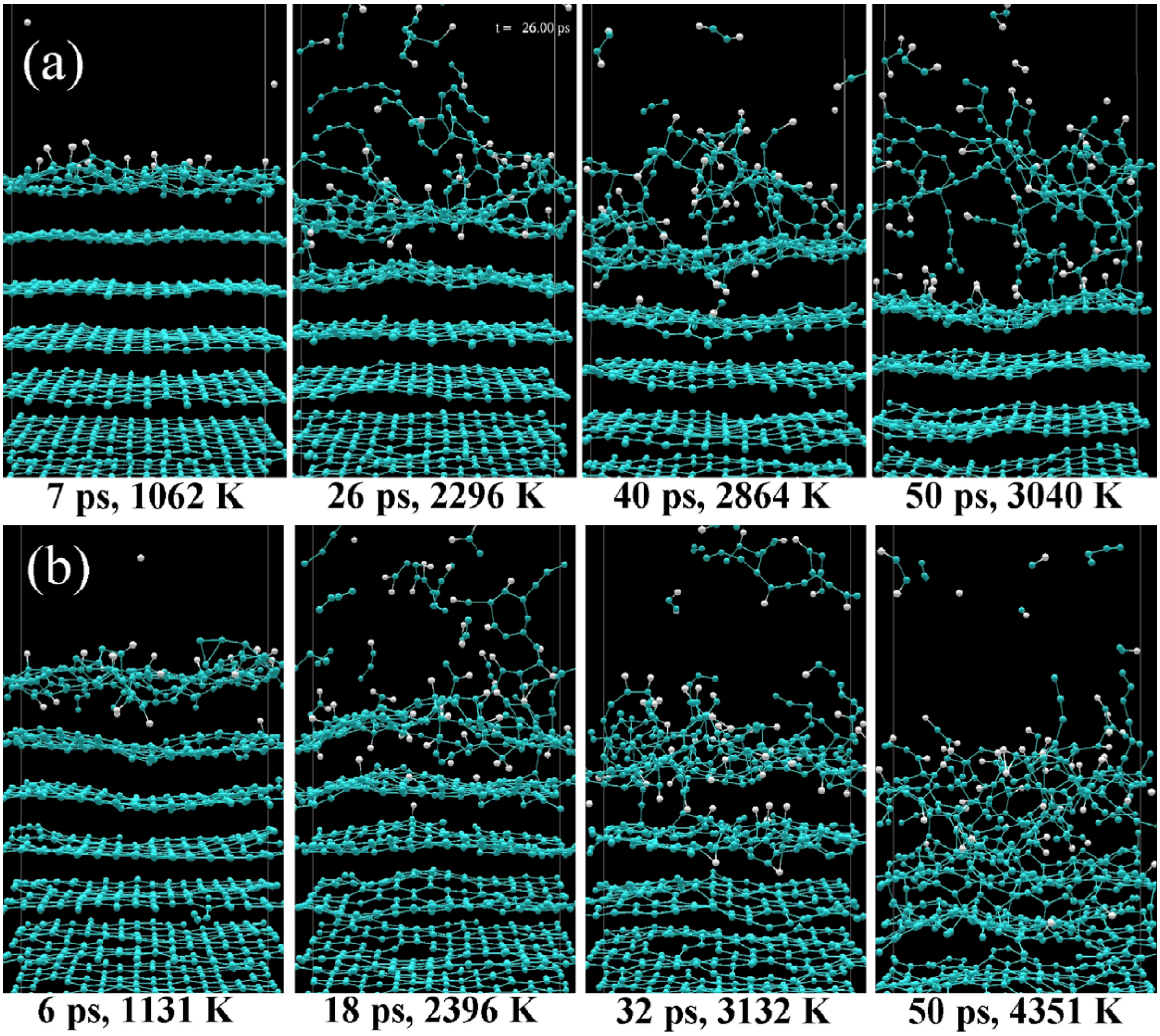

Fig. 2. (a) Snapshot of graphite peeling in case of the graphite of perfect crystal, and (b) snapshot of graphite peeling and amorphization in the case of the graphite including monovacancies.

different point from the case of perfect crystal, covalent bonds were created between under graphene layers. Namely, the graphite including vacancies was amorphized by the hydrogen bombardment.

To estimate the strength of this amorphization, we counted the covalent bond created between the carbon atoms which were members of different layers initially. Here this covalent bond is called ‘interlayer bond’. The interlayer bond refers not only to interlayer covalent bond but also to the covalent bonds which form a molecule composed of carbon atoms from the different layers. Fig. 3 shows the number of the interlayer bonds as a function of elapsed time. The numbers of interlayer bond in the case of the graphite including vacancies were larger than that in the case of perfect crystal. Moreover, the number of interlayer bonds in the case of the graphite including monovacancies was larger than that in the case of the graphite including divacancies. Similar results were observed in the other incident energy less than 5 eV.

We also investigated the hydrocarbon production. When a carbon atom moved into the position at a distance of 12 Å from the initial graphite surface, it was here regarded as a detached carbon atom, for instance that produced C_2H_2 is count as two detached carbon atoms. Fig. 4 shows the total amount of detached carbon

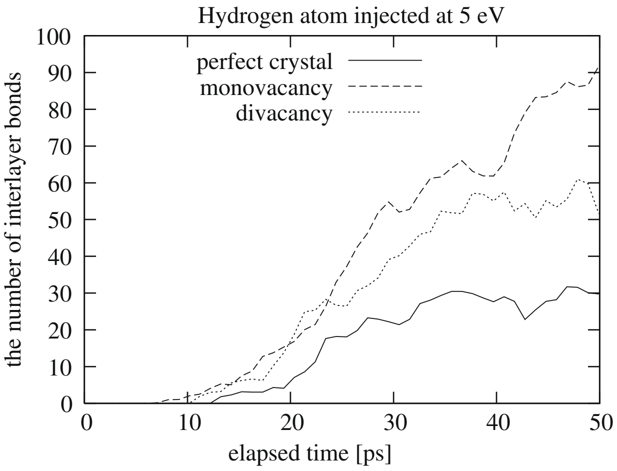

Fig. 3. The numbers of interlayer bonds, which connects between the carbon atoms from initially different layers.

atoms n_c as a function of elapsed time. The total amount of detached carbon atoms n_c increased linearly with the elapsed time and it increase also as the incident energy increased. Using the linear increase of the total amount of detached carbon atoms n_c with the elapsed time, we fitted the total amount of detached carbon atoms $n_c(t)$ to the following function of elapsed time t:

$$n_c(t) = \phi S(t - t_0), \tag{1}$$

where S is the area of the graphite surface $2.00 \times 2.17\ \text{nm}^2$. The coefficient ϕ and the parameter t_0 were regarded as a flux of detached carbon atoms and the time at which the hydrocarbon production starts, respectively. Fig. 5 showed that the flux of detached carbon atoms increased linearly as the incident energy increased. However, the flux of detached carbon atoms ϕ was independent of hydrogen isotopes. The time t_0 decreased as the incident energy increased (see Fig. 6). This results shows deuterium and tritium atoms started detaching carbon atoms earlier than hydrogen atoms.

4. Discussions

In the case of the graphite of perfect crystal, graphite peeling occurred. The graphenes, which was heated up by injection of hydrogen atoms, can move only to the above region because the repulsive force of interlayer intermolecular potential prevents them from approaching under graphenes. On the other hand, the graphite including vacancies was amorphized. We consider that the amorphization is caused by the following mechanisms. First, the interlayer interaction does not occur in the region of a vacancy. That is, a carbon atom in the next graphene layer facing to the vacancy experiences a weaker interlayer repulsive force than the case of the graphite of perfect crystal and then it can approach the next graphene layer. Seconds, carbon atoms around vacancy, which is a sphere painted by white in Fig. 1, has only two covalent bonds. In carbon system, the coordination number of 3 is more stable than the coordination number of 2. Therefore, that the carbon atoms around vacancy prefer to create covalent bond with a carbon atoms in the next graphene layer when the graphene layers approach at the region of vacancy. As a result, the graphite including the vacancy easily changes to an amorphous structure.

By comparison between the cases of graphite including monovacancy or divacancy, we obtain the result that the graphite including monovacancy is more easily amorphized than the graphite including divacancy. From the above consideration, which is that the carbon atoms around vacancy bring about amorphization, we would like to focus attention on the number of the carbon atoms around vacancy, whose coordination numbers are two. Three carbon atoms whose coordination number is two exist around a monovacancy, while four carbon atoms whose coordination numbers are two exist around a divacancy. However, the number of monovacancy is twice number of divacancy in the equal density of carbon atoms. Consequently, the total number of the carbon atoms whose coordination numbers are 2 in the graphite including monovacancy is larger than that in the graphite including divacancy. In our under standing, this facts caused stronger amorphization to the graphite including monovacancy than the graphite including divacancy.

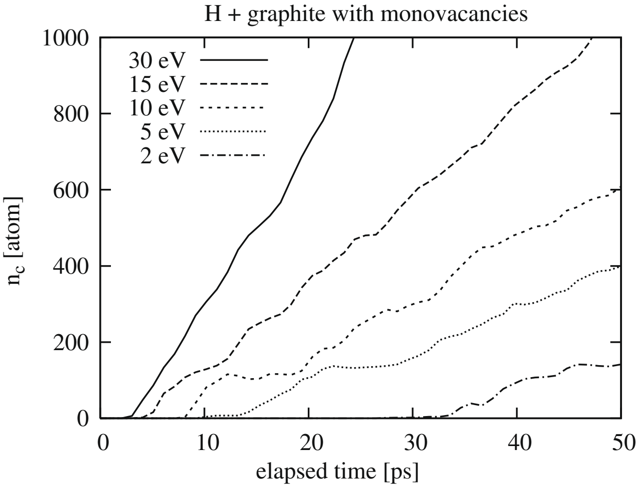

Fig. 4. Total amount of the detached carbon atoms from the graphite surface n_c. Though this figure shows only the case of the graphite including monovacancies, the other cases of perfect crystal and divacancy show similar profiles.

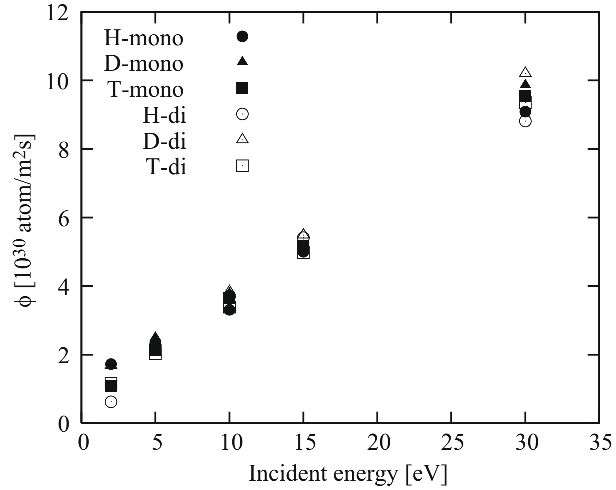

Fig. 5. The flux of detached carbon atoms ϕ as a function of incident energy. The words 'H', 'D' and 'T' indicate hydrogen, deuterium and tritium atoms, respectively. The words 'mono' and 'di' indicate the graphite including monovacancies and divacancies, respectively.

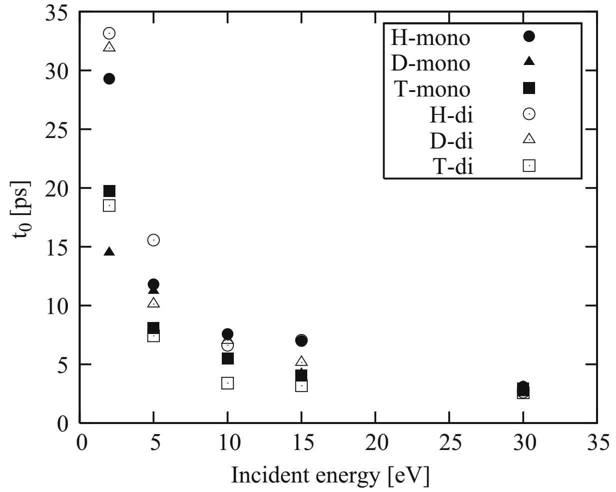

Fig. 6. The time t_0 at which the hydrocarbon production starts as a function of incident energy. The words 'H, 'D' and 'T' indicate hydrogen, deuterium and tritium atoms, respectively. The words 'mono' and 'di' indicate the graphite including monovacancies and divacancies, respectively.

Because chemical interactions are valid only at short range, the hydrogen atom cannot interact chemically with two graphenes simultaneously. The dynamics of hydrogen atoms in the graphite of perfect crystal was explained by three events on a single graphene adsorption, reflection and penetration. The adsorption in the first graphene at the incident energy of 5 eV and reflection by the first graphene at the incident energy of 15 eV is the accordance with the adsorption and reflection of a single graphene. In the case of 30 eV, the hydrogen atom went through the first graphene, which is similar to penetration in the single graphene, and the next event is to rebound from the second graphene, which is regarded as reflection due to the loss of kinetic energy of the hydrogen atom during the penetration at the first graphene. Consequently, the hydrogen atom was intercalated only when the incident energy is higher than the potential barrier on a six-membered ring, which is about 25 eV in the modified Brenner REBO potential.

In contrast, the MD simulation of the graphite including vacancies shows the intercalation of hydrogen atoms in also low incident energy (<15 eV). I would like to emphasize that intercalated hydrogen atoms are mostly located in the back of the first graphene. It is likely that a hydrogen atom injected into the region around a vacancy causes easily back adsorption rather than penetration. This process should be investigated from the study of a single graphene and a hydrogen atom.

The flux of detached carbon atoms increased linearly as the incident energy increased shown in Fig. 5. Though the incident flux of the MD simulations was larger than that of real experiments, the linear increase of flux of detached carbon atoms with the incident energy accorded with experimental results [8].

The dependence on hydrogen isotopes appears in estimation the time t_0 at which the hydrogen atom bombardment start generating hydrocarbon molecules. The time t_0 decreases as the mass of hydrogen isotope increases. Since this dependence stands out in low energy incidence, it is reasonable to suppose that the other dependences on hydrogen isotopes will appear in the case of low incident energy and low incident flux used in experiments. If the incident flux is low, the flux of detached carbon atoms ϕ will also depend on hydrogen isotope such as experiments. Anyway, to fulfill nuclear fusion, the dependence on deuterium and tritium should be investigated by using the MD simulation. Immediate task in the MD simulation is to develop new methods to treat lower incident flux.

5. Conclusion

The chemical erosion due to hydrogen isotopes onto graphite surfaces was investigated by using the MD simulations with the modified REBO and interlayer intermolecular potential models. To show the effect of vacancies, the graphite of perfect crystal and the graphite including mono- or divacancies were prepared. The bombardment of hydrogen atoms into the graphite of perfect crystal caused ‘graphite peeling’, while the bombardment into the graphite including vacancies brought about amorphization. Measuring the number of interlayer bonds, it was found that the graphite including monovacancies experienced amorphization more strongly than the graphite including divacancies. As the incident energy increased, the flux of detached carbon atoms increased linearly. Tritium and deuterium atoms started producing hydrocarbon molecules earlier than hydrogen atom.

Acknowledgements

The authors acknowledge Professor K. Ohya, Professor K. Tanabe, Professor N. Ohno, Mr. K. Inai and Mr. Y. Kikuhara for stimulating discussions. Numerical simulations were carried out by use of the Plasma Simulator at National Institute for Fusion Science. The work is supported by KAKENHI (Nos. 17540384 and 19055005) and Grant-in-Aid for JSPS Fellows (No. 20-3829). YI, SI, and KM acknowledge support by a CREST (Core Research for Evolutional Science and Technology) grant in the Area of High Performance Computing for Multi-scale and Multi-physics Phenomena from the Japan Science and Technology Agency (JST).

References

[1] D.W. Brenner, O.A. Shenderova, J.A. Harrison, S.J. Stuart, B. Ni, S.B. Sinnott, J. Phys.: Condens. Matter. 14 (2002) 783.
[2] A. Ito, H. Nakamura, A. Takayama, J. Phys. Soc. Jpn., 77 (2008) 114602.
[3] A. Ito, H. Nakamura, Commun. Comput. Phys. 4 (2008) 592.
[4] H. Nakamura, A. Takayama, A. Ito, Contribution Plasma Phys. 48 (2008) 265.
[5] A. Ito, H. Nakamura, J. Plasma Phys. 72 (2006) 805.
[6] D.W. Brenner, Phys. Rev. B 42 (1990) 9458 [Errata; 46 (1992) 1948].
[7] M. Suzuki, J. Math. Phys. 26 (1985) 601.
[8] B.V. Mech, A.A. Haasz, J.W. Davis, J. Nucl. Mater. 255 (1998) 153.